DYNAMICS OF PROTONATED ACETONITRILE FORMATION IN $CD_3CN^{+\bullet}$ + CH_3CN COLLISIONS: A CROSSED-BEAM SCATTERING STUDY

Jan ZABKA[a1], Zdenek DOLEJSEK[a2], Inosuke KOYANO[b] and Zdenek HERMAN[a3]

[a] *J. Heyrovsky Institute of Physical Chemistry, Academy of Sciences of the Czech Republic, 182 23 Prague 8, Czech Republic; e-mail: [1] zabka@jh-inst.cas.cz, [2] dolejsek@jh-inst.cas.cz, [3] herman@jh-inst.cas.cz*

[b] *Department of Material Science, Himeji Institute of Technology, 1479-1 Kanaji, Kamigohri 678-13, Japan; e-mail: koyano@sci.himeji-tech.ac.jp*

Received June 19, 1998
Accepted June 23, 1998

Dedicated to Professor Rudolf Zahradnik on the occasion of his 70th birthday.

Dynamics of the elementary protonation reaction in collisions of the acetonitrile cation with acetonitrile was investigated in crossed-beam scattering experiments in the hyperthermal collision energy range 1.17–2.5 eV. The reaction proceeds by three parallel collision mechanisms: direct proton (deuteron) transfer, direct H-atom transfer, and decomposition of an intermediate complex. The relative contributions of the three mechanisms to the formation of the product at T = 2.5 eV are about equal. Analysis of product angular distributions suggests that the geometry of the critical configuration of the decomposing intermediate is prolate, not far from linear.

Key words: Ion-molecule reactions; Protonation; Reaction dynamics; Crossed-beam experiments.

Elementary reactions of a protonated molecular ion formation in collisions of the ion with its parent neutral molecule seem to exhibit a common feature: the product can be formed by three parallel mechanisms, by a direct proton transfer, by a direct hydrogen-atom transfer, and by decomposition of a long-lived intermediate. The relative proportion of the mechanisms depends on the collision energy and on the particular system under study. The competition of the three mechanisms has been demonstrated in studies of CH_5^+ formation in $CH_4^{+\bullet}$ + CH_4 collisions[1] and its isotopic variants[2], and in isotopic variants of H_3O^+ formation in $H_2O^{+\bullet}$ + H_2O collisions[3]. Also, HD_2O^+ formation in $D_2O^{+\bullet}$ + NH_3 collisions[4] by H-atom transfer and intermediate decomposition belongs to this type of processes.

In this communication, we examine an analogous system, the formation of protonated acetonitrile in collisions of the molecular ion with the parent molecule. The motivation for this study comes partly from state-selected experiments, in which the reactivity of the ground and excited state of the ion reactant is being examined[5].

The reactions

$$CD_3CN^{+\bullet} + CH_3CN \rightarrow CD_3CNH^+ + CD_2CN^\bullet \quad (1a)$$

$$\rightarrow CH_3CND^+ + CH_2CN^\bullet \quad (1b)$$

were investigated in crossed-beam experiments. Energy profiles of the products and scattering diagrams were obtained at hyperthermal energies 1.17 and 2.5 eV (center-of mass, c.m.).

In addition, the collision-induced-dissociation process

$$CD_3CN^{+\bullet} + CH_3CN \rightarrow CD_2CN^+ + D^\bullet + CH_3CN \quad (2)$$

was investigated. From the energy profile of the ion product we could show that the primary beam $CD_3CN^{+\bullet}$, formed by impact of 120 eV electrons, contained both the ground state (1^2E) and the excited state (1^2A_1) of the reactant ion.

EXPERIMENTAL

The experiments were carried out on the crossed-beam scattering apparatus EVA II described earlier[3]. Briefly, reactant $CD_3CN^{+\bullet}$ ions were produced by impact of 120 eV electrons on acetonitrile-d_3 gas (Fluka, puriss.) in a low pressure ion source. The ions were extracted, mass analyzed, and decelerated by a multielement electrostatic lens system to a desired laboratory energy of a few eV. The ion reactant beam had an energy spread of about 0.2 eV (FWHM, full width at half maximum) and an angular spread of about 1° (FWHM). The reactant beam was crossed at right angles by a collimated thermal beam of the neutral acetonitrile molecules emerging from a multichannel jet (angular spread of 10°, FWHM). The two beams could be rotated about the collision center in the plane of the detector. Reactant and product ions were detected using a detection slit, energy analyzed by a stopping-potential analyzer, mass analyzed, and registered by a multiplier. Modulation of the neutral reactant beam, phase sensitive detection, and signal averaging was used to deal with background problems. Velocity profiles of the ion products of reactions (*1a*) and (*1b*) (Figs 2a, 2b) were obtained from energy profiles recorded at a specific laboratory scattering angle. The distributions are given in the Cartesian probability density. For the scattering diagrams, the raw data consisted of angular distributions and sets of energy profiles of the reactant and product ions at a series of scattering angles. The scattering diagram was constructed using the well established procedure[6]; it shows the contours of Cartesian probability density of the ion product in dependence on the velocity and scattering angle. Further dynamical quantities (relative differential cross sections, $P(\vartheta)$ *vs* ϑ, product relative translational energy distribution, $P(T')$ *vs* T', were obtained by appropriate integration of the scattering diagrams[6].

RESULTS AND DISCUSSION

Reactant States

The internal energy states of the reactant molecular ions in the reactant beam were identified by investigating the collision-induced-dissociation (CID) process of the ion, reaction (*2*). The reaction is endothermic with ground state reactants[7] by 1.87 eV. Figure 1 shows the velocity profile of the CID product CD_2CN^+ from reaction (*2*) at T = 2.5 eV, measured at the laboratory scattering angle Θ = +3.5°. One may assume that the CID ion product – much heavier than the dissociating D atom – remains practically where the ion reactant was after collisional excitation, and that it thus traces the energy losses in the inelastic collision of the $CD_3CN^{+\bullet}$ with the target. Two distinct energy losses can be discerned. They can be identified with the dissociation processes from the two lowest states of the reactant ion (and their vibrational envelopes), formed by electron impact ionization: the ground state 1^2E and the first excited state[8] 1^2A_1. The range of energies transferred in the inelastic process is shown in the inset of Fig. 1. It corresponds well to dissociations, to the same dissociation limit, of the reactant ion from the two states. The broadening of the distributions is within limits of the energy spreads in the beams and the respective kinetic effects during dissociations. The shape of the velocity distribution is determined by the population of the states[8] and by the cross section for the inelastic dissociation process.

We conclude, therefore, that the reactant beam of $CD_3CN^{+\bullet}$, used in these experiments, contained ions of two distinct groups of internal energy which originate in the ionization process to the ground and the first excited state of the cation. The following

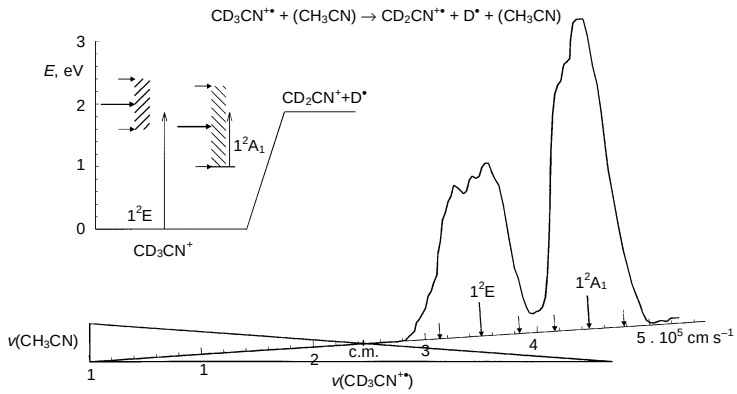

FIG. 1

Velocity profile of CD_2CN^+ from collision-induced-dissociation reaction (*2*) at T = 2.5 eV and Θ_L = +4°. Inset shows the respective energy losses in an energy diagram; arrows in it correspond to arrows in the velocity profile. The underlying structure is the respective Newton velocity vector diagram of the system (c.m. indicates the position of the center of mass)

scattering results refer thus to reactant ions with this internal energy content. The experimental evidence of the existence of reactant ions with these two distinct energy distributions in the reacting ion beam is important in connection with the complementary TPEPICO experiments on the effect of internal energy on the dynamics of reaction (*1*).

Dynamics of the Protonation Reaction

The protonation reaction of acetonitrile is exothermic by 2.73 eV with ground state reactants[7]. Figures 2a and 2b show velocity profiles of the ion products CD_3CNH^+ and CH_3CND^+ from reactions (*1a*) and (*1b*), respectively, at the collision energy of 2.50 eV.

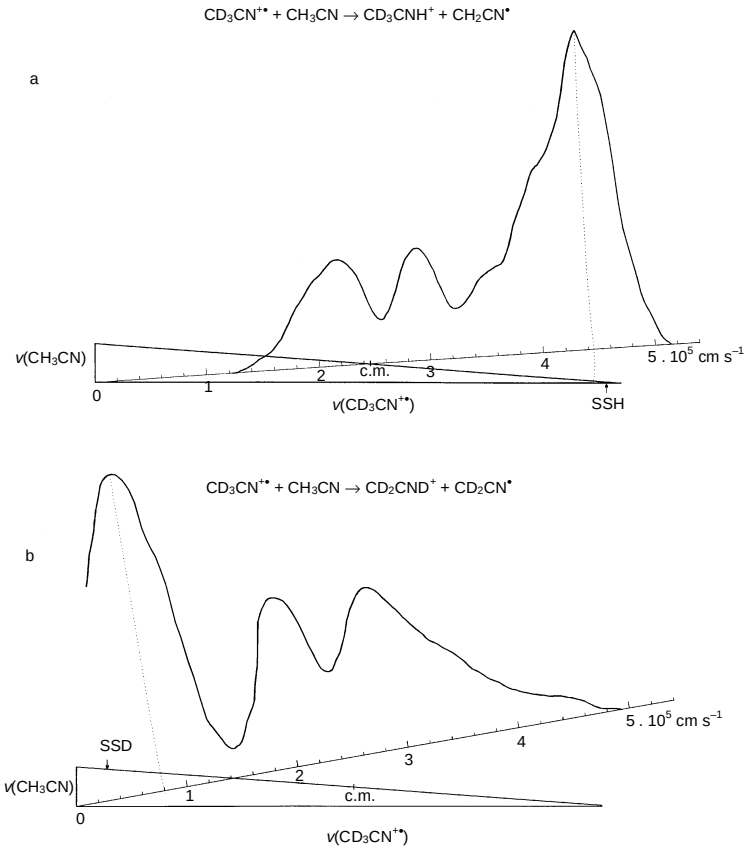

FIG. 2

Velocity profile of the ion product from reaction (*1*) at T = 2.5 eV with an underlying structure of the respective Newton velocity vector diagram (c.m. indicates the position of the center of mass, SSH and SSD the values of product ion velocity for spectator stripping of H and D^+, respectively); profiles in Cartesian probability density. a CD_3CNH^+ from reaction (*1a*) at Θ_L = +4°; b CH_3CND^+ from reaction (*1b*) at Θ_L = +10°

The profile of CD_3CNH^+ shows three distinct peaks:

– a very large peak at almost the reactant beam velocity, with a maximum close to the point of H atom stripping by the reactant ion from the target neutral molecule (SSH);

– two peaks of the same intensity, symmetrically located (within experimental errors) forwards and backwards with respect to the tip of the c.m. velocity vector.

The velocity profile of CH_3CNH^+ shows the following features:

– a strong peak at very low laboratory velocities, in the vicinity of the deuteron stripping by the neutral reactant (SSD);

– two peaks about the same intensity, forwards and backwards with respect to the c.m., analogous in position to the peaks in the CD_3CNH^+ profile.

In addition to the velocity profile of CD_3CNH^+, a full scattering diagram was obtained for this product at the collision energy of 2.50 eV. The scattering diagram is shown in Fig. 3 (the velocity profile in Fig. 2a is the profile along the dashed line). The scattering diagrams exhibits the same features as the profile in Fig. 2a: a prominent forward peak with a maximum close to the stripping of H atom by the reactant ion, and two weaker, symmetric maxima forwards and backwards with respect to the tip of the c.m. velocity vector (marked by cross in Fig. 3).

The scattering diagram makes it possible to derive further dynamical characteristics. Figures 4a, 4b show the center-of-mass angular distributions (relative differential cross

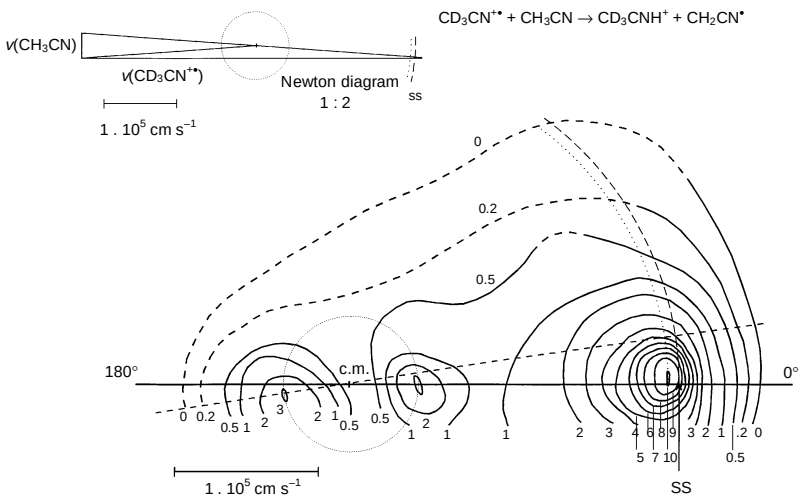

FIG. 3

Contour scattering diagram of CD_3CNH^+ from reaction (*1a*) at T = 2.5 eV; c.m. denotes the position of the center of mass, SS the spectator stripping velocity for H atom transfer, solid line shows the direction of the relative velocity, dashed line the direction along which the velocity profile in Fig. 2a was measured. Inset shows the respective Newton velocity vector diagram (note reduced scale)

sections), $P(\vartheta)$, obtained by the usual integration[6] over the entire scattering diagram (Fig. 4a, open points), and over the scattering diagram with the exclusion of the strong forward peak (Fig. 4a, solid points). This part is shown expanded in scale again in Fig. 4b. The exclusion of the forward peak was obtained by deconvolution of the velocity profiles at specific center-of-mass angles. The angular distribution in Fig. 4b is symmetric with respect to $\vartheta = 90°$, with prominent peaks at 0 and 180°. The ratio $P(0°)/P(90°) = P(180°)/P(90°) = 8$.

Figure 5 exhibits the product relative translational energy distribution $P(T')$, derived from the data in the scattering diagram in Fig. 3. The distribution shows two maxima, one at low energy $T' = 0.15$ eV, and the second at $T' = 2.15$ eV, very close to the translational energy expected for the spectator stripping mechanism ($T' = 2.25$ eV). Integration of the diagram, with the exclusion of the forward peak (and relevant to the angular distribution in Fig. 4b) is shown by solid points. The ratio of the areas below the solid-point curve (area of the first maximum) and the rest of the $P(T')$ distribution gives the ratio of contribution of both channels to the reaction. The ratio is 1 : 6.4.

The velocity profiles in Fig. 2 and the scattering diagram in Fig. 3 show that – similarly as in the earlier studies of protonation reactions between molecular ions and their own molecules[1–3] – three collisional mechanism contribute simultaneously to the formation of the protonated product:

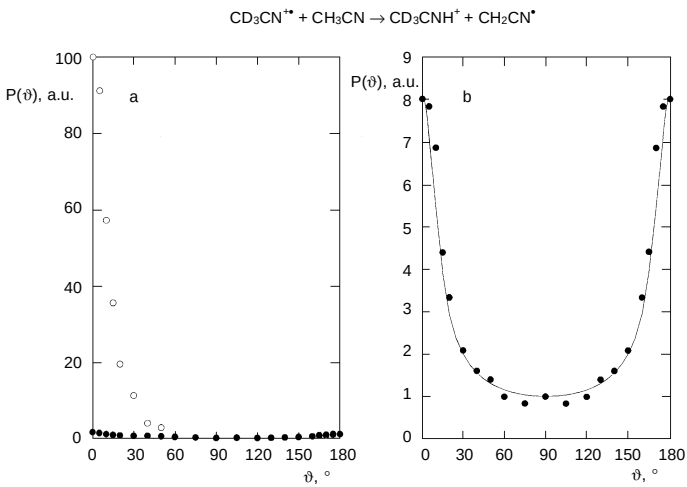

FIG. 4

C.m. angular distributions, $P(\vartheta)$–ϑ, of CD_3CNH^+ from reaction (*1a*) at $T = 2.5$ eV as obtained from the scattering diagram in Fig. 3. a Open points: integration over the entire scattering diagram, solid points: integration with exclusion of the forward stripping peak (complex formation contribution only, in scale); b integration with the exclusion of the forward stripping peak (complex formation contribution) with $P(\vartheta)$ scale expanded, solid line through experimental points shows results of model calculation (see text)

– a direct, H atom transfer mechanism, responsible for the large, forward peak in the velocity profile of CD_3CNH^+ in Fig. 2a and the outer forward peak in the scattering diagram in Fig. 3;

– a direct deuteron-transfer mechanism, responsible for the low-velocity peak of CH_3CND^+ in Fig. 2b (backward with respect to the c.m.);

– decomposition of an long-lived intermediate complex which shows up as the inner pair of symmetrical forward- and backward-scattered peaks in both velocity profiles and the scattering diagrams (Figs 2a, 2b and 3).

The direct mechanisms exhibit the characteristics of the stripping mechanism: the product peaks in the vicinity of the c.m. velocity which corresponds to a simple momentum transfer of the transferred particle ($H;D^+$) to the projectile ($CD_3CN^{+\bullet}$, CH_3CN, respectively). The process can be described as a concerted dissociation of the old bond and simultaneous formation of the new bond in a collision of a typical duration comparable to a vibrational period. The stripping mechanism requires that a specific fraction of the relative energy is channeled into the translational energy of the products. The high-energy peak in the $P(T')$–T' plot in Fig. 5 corresponds well to the prediction of the stripping, H atom transfer mechanism.

The mechanism of intermediate-complex decomposition gives rise to a forward-backward symmetry of the respective part of the scattering pattern which results from a formation and subsequent dissociation of an intermediate species of a mean lifetime of at least several rotations of this species. In the present case,the mean lifetime can be

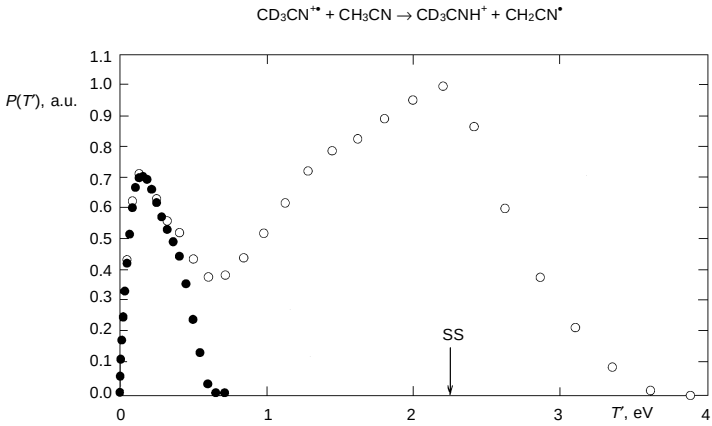

FIG. 5

Translational energy distributions of products of reaction (*1a*), $P(T')$–T', at T = 2.5 eV. Open points refer to integration over the entire scattering diagram in Fig. 3, solid points: integration with the exclusion of the stripping contribution (complex formation contribution only); SS denotes translational energy expected for product formed by ideal spectator stripping mechanism

estimated to be longer than about $5 \cdot 10^{-12}$ s. During this time the energy of the complex can be statistically redistributed over the internal degrees of freedom; the average energy which goes into translation is then much smaller that the most probable energy connected with the impulsive stripping mechanism. The low-energy peak in the $P(T')$–T' distribution in Fig. 5 is evidently connected with translational energy release in the intermediate complex decomposition. From the results one can estimate the relative contributions of the three mechanisms to the product formation. From the ratio of the areas under the curves in Fig. 5 (6.4 : 1, as mentioned earlier) one can estimate the contribution of the H atom transfer direct process and part of the contribution to the complex formation. Assuming statistical H/D scrambling in the complex, this part is 1/5 of the total contribution of the complex formation mechanism. From comparison of Figs 2a, 2b and 3, assuming the same angular distribution for CH_3CND^+ formed by direct D^+ transfer and for CD_3CNH^+, formed by H atom transfer, one can roughly estimate that the contribution of the D^+ transfer mechanism and the H atom transfer mechanism is about equal. Thus the relative contributions of the three mechanisms to the product formation, direct D^+ transfer to direct H atom transfer to complex formation are about equal.

The shape of the c.m. angular distribution pertinent to the complex formation mechanism contains information on the geometry of the critical configuration of the dissociating complex[9] (the critical configuration is defined as a configuration of the intermediate from which it dissociates by an extension of a critical bond). This distribution is shown in Fig. 4b. The strong peaking of the distribution at 0 and 180° suggests for the critical configuration of a prolate geometry, not far from linear. The moments of inertia of the critical configuration, treated as a rotating near-symmetric top, could be estimated from the angular distribution shape. We applied the earlier developed procedure[9] to the analysis of the angular distribution in Fig. 4b. The calculated shape is shown by solid line through the points and the model requires a critical configuration geometry with a reduced moment of inertia $I_R = I_1 I_2/(I_1 - I_2) = 7.1$; this correspond to the ratio of the moments of inertia $I_2/I_1 = 15$ (I_1 is the moment of inertia about the symmetry axis along which the complex comes apart, I_2 is the moment of inertia about the axis perpendicular to it).

Evidently, the complex may assume during its lifetime various configurations. Preliminary considerations[10] indicate that a configuration $[CD_3CN–NCCH_3]^{+\bullet}$ may be of a considerable stability. Hydrogen–deuterium scrambling points to involvement of cyclic structures, too. The scattering experiments suggest that the critical configuration has a very prolate geometry, presumably with the transferred hydrogen bonded to nitrogen atom of the product ion to be formed. The protonation reaction is very exothermic (2.73 eV). The observed participation of the complex-formation mechanism implies that there is a substantial well on the potential energy surface. This in turn means that either the dissociation energy of the intermediate, with respect to the reactants, is 3–4 eV

(unusually large for a molecular ion-molecule species) or that the products are formed in excited states. In the system $CH_4^{+\bullet}$–CH_4, studied earlier[1], a dynamical information on the existence of thermodynamically stable intermediate $C_2H_8^{+\bullet}$ was obtained. Theoretical calculations on the stability of such a species[11,12] provided an important argument in the elucidation of the collisional dynamics of this system. Analogous calculations on the system acetonitrile cation–acetonitrile would be of great interest.

This work has been supported by Czech-Japanese cooperation grants of the Ministry of Education, Sports and Youth of the Czech Republic Kontakt No. ES 017(1996) and No. ME 188(1998) and by the research grant No. 203/97/0351 of the Grant Agency of the Czech Republic. One of the authors (Z. H.) acknowledges with pleasure fruitful discussions with R. Zahradnik on this and numerous earlier occasions.

REFERENCES

1. Herman Z., Henchman M., Friedrich B.: *J. Chem. Phys*. **1990**, *93*, 4916.
2. Herman Z., Tanaka K., Kato T., Koyano I.: *J. Chem. Phys*. **1996**, *85*, 5705.
3. Vancura J., Herman Z.: *Chem. Phys*. **1991**, *151*, 249.
4. Vancura J., Herman Z.: *Collect. Czech. Chem. Commun*. **1988**, *53*, 2168.
5. Fukuzumi T., Koyano I.: *Reports of Faculty of Science, Himeji Institute of Technology* **1994**, *5*, 9.
6. Friedrich B., Herman Z.: *Collect. Czech. Chem. Commun*. **1984**, *49*, 570.
7. Lias S. G., Bartmess J. E., Liebman J. F., Holmes J. L., Levin R. D., Mallard W. G.: *J. Phys. Chem. Ref. Data* **1988**, *17*, Suppl. No. 1.
8. Kimura K., Katsumata S., Achiba Y., Yamazaki T., Iwata S.: *Handbook of HeI Photoelectron Spectra of Fundamental Organic Molecules*. Japan Scientific Societies Press, Tokyo 1981.
9. Sadilek M., Herman Z.: *J. Phys. Chem*. **1993**, *97*, 2147.
10. Zahradnik R.: Unpublished results.
11. Havlas Z., Bauwe E., Zahradnik R.: *Chem. Phys. Lett*. **1985**, *121*, 330.
12. Kamiya K., Morokuma K.: *Chem. Phys. Lett*. **1986**, *123*, 331.